From Pixels to 3D Representations of Buildings:
A 3D Geo-visualization of Perspective Urban Respecting Some Urbanization Constraints

Rani El Meouche[1][a], Mojtaba Eslahi[1], Anne Ruas[2] and Muhammad Ali Sammuneh[1]

[1]Institut de Recherche en Constructibilité (IRC), ESTP Paris, 28 Avenue du Président Wilson, 94230 Cachan, France
[2]LISIS/ IFSTTAR, Université de Marne-la-Vallée, 5 Boulevard Descartes, 77420 Champs-sur-Marne, France

Keywords: 3D Modelling, GIS (Geographic Information System), CA (Cellular Automata) Model, Urban Sprawl, Urban Growth, SLEUTH Urban Growth Model, Building Footprints.

Abstract: In this paper, we generate the fictive 3D buildings and provide a 3D representation of an urban growth model using ArcGIS. SLEUTH urban growth model, like the other CA (Cellular Automata) models, creates a prospective 2D map containing some pixels on which urbanization is supposed to occur. These pixels have to be transformed into 3D building representations, while respecting some restrictions on urbanization. To create a building from a pixel, we transform the pixels from raster data to building footprints. In the process of transformation, different considerations and constraints are considered such as the direction of the footprints and the distances to urban objects and geographic features. To generate the 3D representations of the buildings, the appropriate heights are added to these footprints. The height of the buildings depends on the probability of the height of adjacent buildings. Although the provided 3D model is a primary and simple model, the 3D representation of the urban growth allows having different images of the city of tomorrow for supporting the scientists and authorities in charge of urban planner and management.

1 INTRODUCTION

In recent years, various researches on 3D virtual city models have been carried out. 3D city models are used to represent the urban surfaces and the important objects attached to them, including the buildings and the environment for different purposes such as communication, management of urban heritage, urban planning projects, and simulation modeling in terms of noise, solar, pollution, climate changes, flooding and urban sprawl (Shiode, 2000; Kolbe and Gröger, 2003; Zhu et al., 2009; Billen et al., 2012; Billen et al., 2014; Biljecki et al., 2015).

There are different techniques to generate a 3D city model, such as 3D building creation from urban footprints (Ledoux and Meijers, 2011; Pedrinis and Gesquière, 2017; Chaturvedi et al., 2019) and 3D reconstruction and data integration that are used in merging photogrammetry or laser scanning with GIS data (Haala and Kada, 2010; Kapoor et al., 2010; Hervy et al., 2012; Billen et al., 2012; EL Meouche et al. 2013; Tomljenovic et al. 2015, Pepe et al., 2019).

Nowadays, there are different tools for generating a 3D model in different fields of architectural, industrial, mechanical and electronical engineering such as Maya, 3ds Max, Auto CAD, Sketch Up, Unity, City Engine and ArcGIS. In this research, the 3D buildings are created by giving the third dimension to 2D footprints of the buildings. The third dimension indicates the height of the buildings that is obtained according to the buildings' class and population density. The buildings are illustrated in block models with flat roof structure (similar to LoD1 of CityGML). We have used ArcGIS 10.6 for our 3D modeling process. GIS based applications let us creating the 3D buildings and analyzing geographic information. The objective here is to illustrate the 3D representation of an urban growth model while respecting a set of constraints.

In this paper, we have used the SLEUTH urban growth model, and visualized the obtained 2D results on 3D. SLEUTH is an inductive pattern-based model

[a] https://orcid.org/0000-0001-5063-6638

that uses cellular automata and terrain mapping. This model employs some growth rules to address urban growth model, and it is widely used to simulate the urban growth (Clarke, 2008; Project Gigalopolis, 2018; Eslahi et al. 2019). SLEUTH's acronym is derived from its data input requirements: Slope, Land use, Exclusion, Urban, Transportation and Hillshade.

The SLEUTH results are limited to some raster data that are difficult to interpret for decision makers. The results are some pixels on which urbanization is supposed to occur, while they do not make much sense from urbanism point of view. Therefore, we have proposed to transform the pixels into 3D building representation and to place them in all of the available spaces. The objective of this paper is not to explain the SLEUTH model, but to give an idea to transfer the 2D pixels, obtained from SLEUTH, to 3D representations of the buildings.

In the next section, the study area is presented. The procedure of transforming a pixel to a 3D representation of a building is described in section 3. A 3D visualization of the urban growth model is provided in section 4. The paper is concluded in section 5.

2 STUDY AREA

The proposed model has been applied in three study areas with different scales including metropolis, a city and a rural area. Due to the ease of visualization, the application of the model to the smallest study area is presented in this paper. The study area is Rieucros, a small community in a rural area that is located in the department of Ariege in south of Toulouse, France (43° 05′ 07″ North, 1° 46′ 04″ East) (see figure 1). The extent of the study area is 400 ha with 686 inhabitants (Legal populations, INSEE - national institute of statistics and economic studies, France, 2016).

Geospatial database and geographic information systems are applied to create the input maps of SLEUTH. All the maps have the size of 100×100 pixels that feature a cell size of 20m×20m (~400m2).

Slope and hillshade maps are derived from Digital Elevation Model (DEM) of RGE ALTI with a spatial resolution of 5m, provided by IGN (national institute of geographic information and forestry).

Urban areas, excluded areas and transportation maps are generated automatically from BD TOPO and BD ORTHO from IGN database of 2017. Urban map is classified into two classes of urban and nonurban. To create the urban maps, the undifferentiated buildings with more than 3m height and more than 50m^2 surfaces are used.

Figure 1: Location of the study area of Rieucros.

The compound annual population growth rate is calculated and the average population for the coming years (2050) is estimated for the study area. Using SLEUTH urban growth modelling, we define different urban fabric scenarios based on socio-demographic data, which are integrated into the model during 2D simulations (Eslahi, 2019).

3 FROM PIXEL TO 3D BUILDING REPRESENTATION

As discussed before, we have used a CA model to simulate the forecasting urban growth for our study areas. Here, we aim to create the 3D building representation from the pixels.

The distances from the constraints and the neighbourhoods of geographical objects are not explicitly considered in CA models. Therefore, we have used the topographic objects such as buildings, rivers, excluded areas and the current buildings, and make a set of constraints. Considering these constraints, we have created the footprints of the buildings and then we have given them the value of the height according to the urban fabric scenarios.

In order to visualize the SLEUTH results in three-dimensional space, first, the pixels need to be transformed from raster data to building footprints. The number of the buildings that can be located in each pixel depends on the pixel size and the surfaces of the buildings. An average surface for each type of building is calculated based on the average surface of current buildings. Afterwards, appropriate heights are

added to these footprints. The heights are based on the adjacent buildings. In the process of transformation of the pixel to building footprints, different considerations and constraints are considered, such as the direction of the footprints and the distances to urban objects and geographic features. The distance of the new building to the urban objects and geographic features (e.g. current buildings, roads, railways, rivers, vegetation, cemeteries, airfields, activity areas) are obtained from the average distances of the existing buildings to them.

The procedure of generating a 3D building representation from a pixel is presented in figure 2.
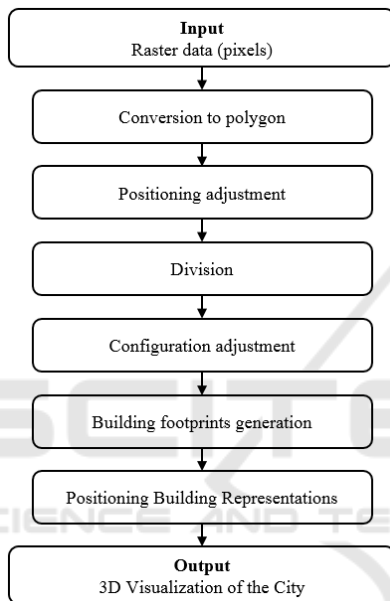

Figure 2: The 3D building representation generation procedure.

As it is illustrated in figure 2, in order to create a 3D building model, the pixels have to first, change to polygons that indicate the buildings footprints, and take the value of heights. To transform a pixel to a polygon, the SLEUTH output maps (the raster data that are derived from SLEUTH simulation) should be georeferenced and converted to vector data. This provides the polygons instead of each pixel, which simplify the processing (see section 3.1). Next, each polygon is oriented along its nearest road section. The polygons are divided to four squares. This is because in our algorithm the position of the building respects certain distances from urban objects and geographic features. If these distances are not observed, the polygon will be removed. Therefore, by dividing a polygon into smaller squares, we decrease the risk of losing the whole polygon (see section 3.2).

The urban objects and the geographic features define some constraints for a polygon. These constraints cause the configuration of the polygons to be adjusted. We have defined two type of constraints including linear constraints (e.g. roads, rivers and railways) and discrete constraints (e.g. cemeteries, airport, and existing buildings). The difference of these two constraints is on the calculation of the average distances of the current buildings to them. The pixels that were turned along their nearest road sections make the overlaps of the polygons that are adjacent each other. Therefore, in this step the overlaps and the parts of the polygons that are close to the constraints will be removed (see section 3.3).

In next step, the small squares that are identified as a polygon are assembled taking into account the average area of the current buildings. The surfaces are set according to the scenarios by making an erosion to achieve the desired footprints for each building (see section 3.4 and 3.5).

The process of calculation the building's height is done, in parallel to building footprints generation. We have calculated the surface of each building footprints. In the cases that the surfaces are too small to be on the upper building class, we give the height according to their surfaces. Other footprints take the height of the nearest neighbours, until the rate of the building classes that are defined will be filled. The process of giving height to the building footprints will be explained in detail in section 4.

3.1 From Pixel to Polygon

The SLEUTH outputs include the non-geo-referenced raster that contains three types of pixels representing the current urban area, new urban area and null pixels. The purpose of this step is to geo-reference this raster data with respect to our database vector data. This process is based on a polynomial transformation. It renders the Root Mean Square deviations (RMS) as a control index, which in general, must be below the size of a pixel.

Later, the raster data is converted to vector data to facilitate the processing. In fact, we have extracted raster data from shape files (vector data) for creating the input maps of SLEUTH and now, we do the inverse function.

3.2 Positioning and Division of the Building Footprints

After preparing the output of the SLEUTH model for 3D procedure, in this section, the generated polygons, should be rotated along the closest road section. The

orientation is done based on the size of the polygon and the coordinates of its centre (Xc, Yc). The orientation is made with respect to the nearest road section (see figure 3).
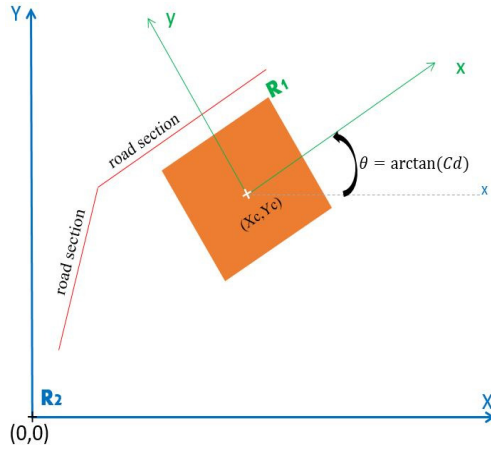

Figure 3: Orientation of a polygon, R1 and R2 are the local and overall references respectively.

The roads are divided into the small sections, then, their directing coefficient (Cd) is calculated with the bellow equation:

$$Cd = \frac{Ye - Ys}{Xe - Xs} \qquad (1)$$

where *(Xs,Ys)* and *(Xe,Ye)* are respectively the start and the end coordinates of the section. Then, the angle of orientation of the road section is calculated according to the horizontal axis in two cases:

Case 1, if Xe-Xs = 0 (section parallel to vertical axis):

$$\Theta = \pi/2 \qquad (2)$$

Case 2, if not:

$$\Theta = \arctan (C_d) \qquad (3)$$

Finally, the squares are oriented using this angle by associating each oriented polygon to a local coordinate system, considering the coordinates of the corners of the polygons in the overall reference. Therefore, the solution becomes a simple change of reference in the plane. The rotation according to Z is as follows:

$$R_z = \begin{bmatrix} \cos\Theta & -\sin\Theta & 0 \\ \sin\Theta & \cos\Theta & 0 \\ 0 & 0 & 1 \end{bmatrix} \qquad (4)$$

The change is made according to the following equation. The angle calculated in the counter clockwise direction.

$$\begin{cases} X = Xc + x\cos\Theta - y\sin\Theta \\ Y = Yc + x\sin\Theta + y\cos\Theta \end{cases} \qquad (5)$$

where (x, y) are the coordinates of the corners expressed in local coordinate system and (X, Y) their associates in global coordinate system.

$$\begin{cases} X = Xc + \left(\dfrac{R}{2}\right)(\cos\Theta - \sin\Theta) \\ Y = Yc + \left(\dfrac{R}{2}\right)(\sin\Theta + \cos\Theta) \end{cases} \qquad (6)$$

Afterwards, we change the sign of the cosine and sine for the coordinates of four corners.

Corner 1:

$$\begin{cases} x = \dfrac{R}{2} \\ y = \dfrac{R}{2} \end{cases} \rightarrow \begin{cases} X1 = Xc + \left(\dfrac{R}{2}\right)(cos\,\Theta - sin\,\Theta) \\ Y1 = Yc + \left(\dfrac{R}{2}\right)(sin\,\Theta + cos\,\Theta) \end{cases} \qquad (7)$$

Corner 2:

$$\begin{cases} x = \dfrac{R}{2} \\ y = -\dfrac{R}{2} \end{cases} \rightarrow \begin{cases} X2 = Xc + \left(\dfrac{R}{2}\right)(\cos\Theta + \sin\Theta) \\ Y2 = Yc + \left(\dfrac{R}{2}\right)(\sin\Theta - \cos\Theta) \end{cases} \qquad (8)$$

Corner 3:

$$\begin{cases} x = -\dfrac{R}{2} \\ y = -\dfrac{R}{2} \end{cases} \rightarrow \begin{cases} X3 = Xc + \left(\dfrac{R}{2}\right)(-\cos\Theta + \sin\Theta) \\ Y3 = Yc + \left(\dfrac{R}{2}\right)(-\sin\Theta - \cos\Theta) \end{cases} \qquad (9)$$

Corner 4:

$$\begin{cases} x = -\dfrac{R}{2} \\ y = \dfrac{R}{2} \end{cases} \rightarrow \begin{cases} X4 = Xc + \left(\dfrac{R}{2}\right)(-\cos\Theta - \sin\Theta) \\ Y4 = Yc + \left(\dfrac{R}{2}\right)(-\sin\Theta + \cos\Theta) \end{cases} \qquad (10)$$

In order to both, considering the constraints and preserving the surfaces of the polygons as much as possible, the polygons are divided into four smaller squares. Therefore, if constraints drive the model to delete a polygon, the algorithm will delete a small square, which meet the restrictions, instead of whole polygon.

3.3 Configuration the Building Footprints

After orienting a polygon, some overlaps occur between them and other layers of the land occupation. In addition, it is necessary to define a distance

between a polygon (which will define the new buildings representation) and the different land occupation entities. The adjustment and positioning of new buildings follow the layout of the old buildings. Therefore, we apply the situation of existing buildings on the polygons in order to create new buildings that would respect the distance between buildings, and the distance to the river, and railways. As mentioned before, two types of constraints are taken into account:

- The constraints that have a linear distribution in space including vegetation, water, roads and railways.

- The discrete constraints that can be modelled by points or small areas including remarkable buildings, cemeteries, airfields, sport grounds, activity areas, industrial or commercial areas and existing buildings.

The logic of these two types of constraints bases on finding the nearest neighbour and respecting the distances similar to it. The only difference is the definition of the notion 'nearest' between linear and discrete constraints.

To explain the method of defining linear constraints, we have used the following example of the river. This method is essentially based on a double geo-processing buffer as follow:

- First, we measure the distance from the nearest existing building to the river (Dr), then we make a buffer of ten times of this distance ($10 \times$ Dr). We assume that all the buildings close to the sections of the river are at this distance (second buffer), which means the buildings that are at the edge of the river.

- The average distance of these buildings from the river is then calculated (the average distance of the buildings located in the second buffer). This average is considered as a minimum distance for new buildings of the riverbank.

For other linear constraints, the similar procedure is done. In these cases, the distance of the nearest building to each road section is measured and it is considered as an average distance for new buildings.

To apply linear constraints to the polygon, the algorithm makes a second buffer with a distance equal to the average distance and remove the intersection of this buffer with the polygon. As mentioned earlier, one of the advantages of dividing polygons into smaller squares is that when we want to remove the intersection of polygons with a buffer,

only the small squares that are within a buffer constraint are eliminated. When only a part of a polygon intersects with the buffer, this subdivision can help the model not to lose the polygon completely. In addition, a threshold for the intersection of a square to a buffer is defined. This threshold is equal to 30% of a square area that intersects with the buffer. It means, if a buffer overlaps more than 70% with a square, that square is deleted. Figure 4 illustrates the sample of the linear constraints definition.
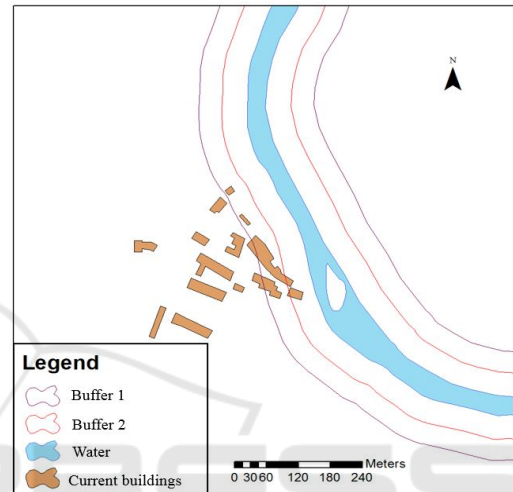

Figure 4: Definition of river proximity constraint.

The discrete constraints are defined by the undifferentiated buildings, industrial buildings and some special spaces (i.e. excluded area, remarkable buildings, cemeteries, airfields, activity areas). In order to taking into account the distance of a polygon from the discrete constraints, it is required to measure the distance of the current buildings from each other and from other discrete constraints. After obtaining the average distance for the current buildings, this distance is applied to the nearest discrete constraints for each polygon. Therefore, a buffer of the average distance is generated that defines the constraint of the existence of a building or a special place. Afterwards, the same argument for eliminating intersections as for linear constraints applies to discrete constraints.

As discussed, in orientation each polygon rotates parallel to the closest road section. In the cases that two polygons are located next together, if the road orientation is changed, one polygon overlaps with part of the other. Therefore, this part of the overlap should be deleted from one of the polygons. The amount of the overlap depends on the angle of change of the road direction from one section to another. The more the road turns, the greater the overlap becomes.

In this step, the division of pixels plays an important role and the small square from one polygon, which overlaps with another, is removed. Therefore, we have created distances between the polygons while avoiding the problem of the superposition.

3.4 Building Footprints Generation

After considering the required distance from the constraints, in this section we have created the building footprints. In previous section, the polygons were divided to small squares. Here, in order to generate the footprints these squares are assembled according to the building types.

The idea is to build building footprints with the surfaces remain among the small squares. We have defined maximum of different areas (Smax) for the new building footprints concerning the type of the buildings and the size of the polygons. Two types are considered for the study area including: the single dwelling and shop top housing, with the Smax of $156m^2$ and $256m^2$ respectively. The squares are assembled according to Smax of each study area.

To make the footprints of buildings we should first, assemble small squares (with same IDs), while checking if the total area exceeds the maximum defined area relative to each scenario (Smax). If the area of the assembled squares were less than Smax, the whole polygon represents one building. Then, we build a layer that contains only the polygons whose surfaces exceed Smax. For these polygons, we return to the state of the decomposition. We gather the two small squares which belong to the same subpixel (the square of the first division) but which are both to the left or the right of the set of small squares of the sub-pixel, i.e. LU (Left/Up) with LD (Left/Down) and RU (Right/Up) with RD (Right/ Down).

This combination is chosen because in our algorithm we assume that the width of a building locates on the side of the road. Since the polygons are oriented towards the road, the sub-squares which facing the road are chosen in such a way that they carry the 'U' (Up). In the case that we assemble the two squares, which bring 'U' together and the two others bring 'D' together, we will have a house facing the road and one behind the other. Therefore, the both buildings will have access to nearest road.

3.5 Positioning Building Representations

The urban fabric scenarios are based on one or the combination of the building types considering the density of the population. After assembling the

squares, we have defined the different possible types of the footprints considering an erosion to each polygon according to their surfaces and building types (see figure 5). Therefore, we have obtained the desired surface for the building footprints as well as respecting the Smax and the distances between the new buildings. Defining different footprints is used in next step to create the 3D representation of the prospective urban map.
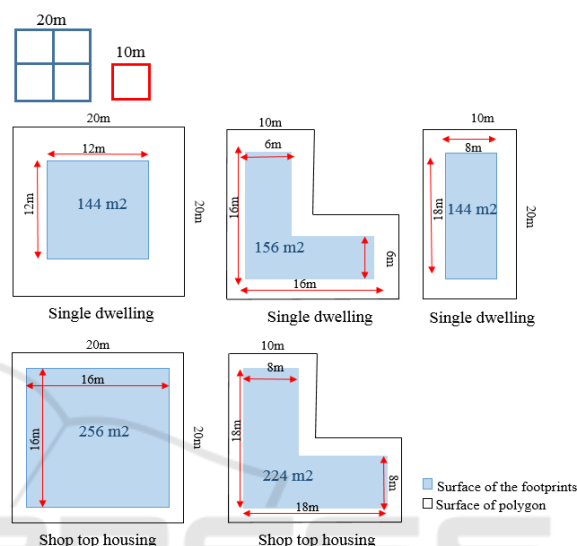

Figure 5: Building footprints by making different erosion to each polygon according to building type.

Now, we have calculated the different probabilities for each polygon according to its neighbourhood building types. These gives the information of the possible height for the new buildings. Given the scenarios where it is necessary to have mixed height values according to predefined percentages associated with each height, we use an algorithm that combines the random aspect and a statistical interpolation.

According to urban fabric, we have two types of buildings that have two different heights. In our algorithm, we ordered the buildings in ascending order of their surfaces (SB1<SB2). For each building types of B1 and B2, their percentages of combination in the scenarios are defined by Prs1 and Prs2, respectively. P1 and P2 indicate the average height probabilities for each building that are calculated from the nearest current building's height. To do this, it is needed to classify the new building according to the distance to the neighbour as follow (see figure 6):

- Class1: New buildings that have at least one neighbour that is part of the current buildings on a circle (r1)

- Class2: New buildings that have at least one neighbour that is part of the current buildings on a limited ring between the small circle (r1) and the large circle (r2)

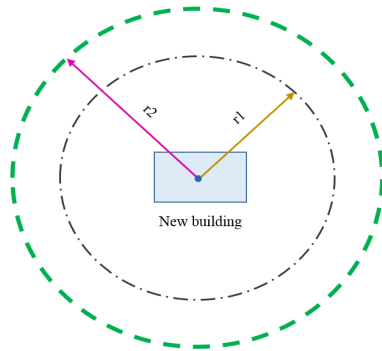- Class3: New buildings that have no neighbours that are part of the current buildings on a circle (r2)

Figure 6: Searching for the nearest neighbour.

The values r1 and r2 are the radiuses that are calculated from the distance of the nearest neighbour of each existing building and apply the quintile classification. We have calculated the distance between the new building and the current buildings, which is in the spaces that is defined by the class (DIS), then the inverse distance (IDIS) and the sum of the inverse distance (SIDIS). Then after, we have computed the influence weight of the type of each building on the type of the new building (building with height equal Hi). Finally, we have deduced the total probability of each type associated with this building and we have obtained a new Pi that signify the probability of a building with height Hi.

In next step, the buildings are divided in two classes according to their types. We have calculated the initial percentage (Pri) of each type for the variable percentage (Pr):

- The buildings that have the surface SB1 associated with the height, H1 (Pr1 = Pri1, Prs1)

- The buildings that have the SB2 surface associated with the height, H2 (Pr2 = Pri2, Prs2)

Therefore, three different percentages for each type of building are calculated including:

- Initial percentage: fixed

- Variable percentage: variable

- Desired percentage: goal

Then, we have tried to adjust the current percentage so that it is very close to the percentages entered by the user of the model according to the diagram that is illustrated in figure 7.

4 3D VISUALIZATION OF THE CITY OF TOMORROW

After, generating the footprints and estimating their related heights, in this section we have illustrated the 3D representation of the model. In order to visualize the 3D model of the city, we have first created the Digital Elevation Model (DEM) using BD TOPO data altitudes (IGN). The results are displayed in ArcScene by making an extrusion of the various layers including new buildings using the height calculated in the previous section. The model is first implemented on the map of the year 2000 to obtain the results of 2017. The accuracy of the model is evaluated by comparing the observed map and the simulated result for 2017. Figure 8 illustrates the 3D representation of Rieucros for 2050.

5 CONCLUSIONS

SLEUTH urban growth model generates the prospective 2D maps containing some pixels on which urbanization is supposed to occur. These 2D maps are limited to a raster data that are difficult to interpret for decision makers and are needed to be transformed into 3D building representations.

In this research, we have proposed an algorithm to transform the SLEUTH results (pixels) into 3D building representations concerning the density of population, urban fabric and some restrictions on urbanization such as the direction of the footprints and the distances to the urban objects and geographic features. The building height depends on the probability of the height of adjacent buildings according to the urban fabric.

The model is applied on the simulated urban growth maps of 2050 for Rieucros. Although the provided 3D model is a primary model, it helps to better understanding of the simulation results and to facilitate the interpretation of the SLEUTH simulation.
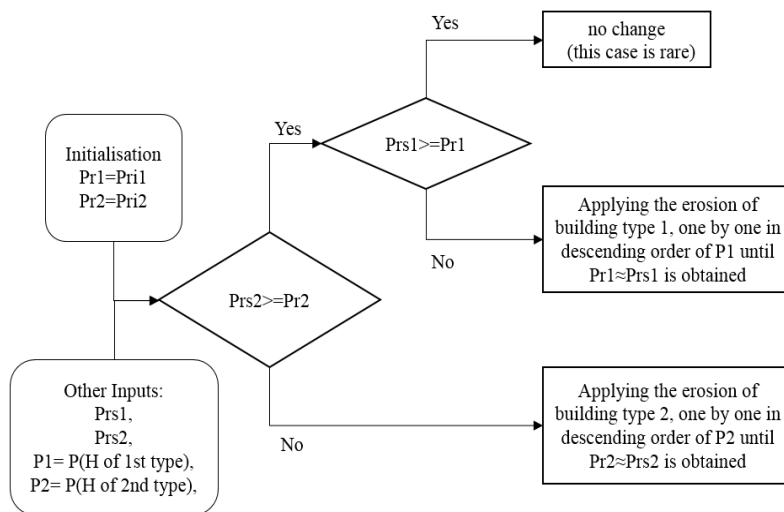
Figure 7: The algorithm of calculating the probability of the height for each building according to the building types and urban fabric scenario.
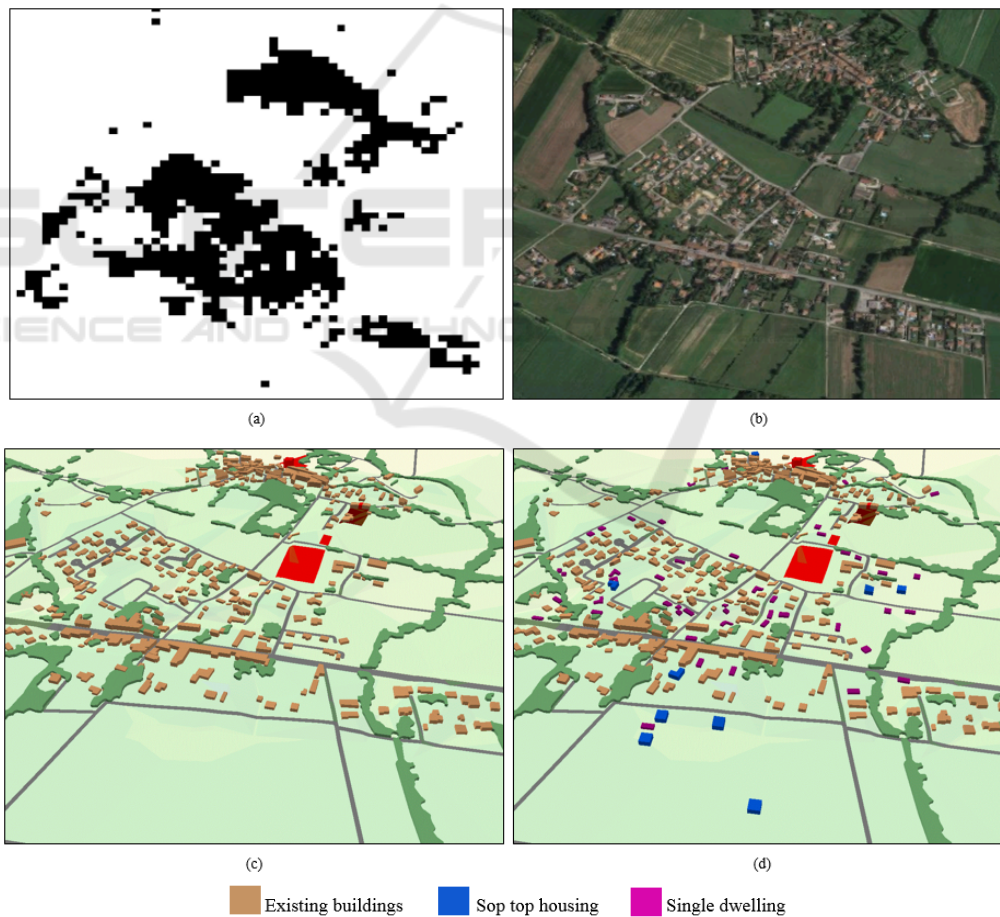

Figure 8: (a) 2D simulated urban map for 2050, (b) Ortho-photo 2017, (c) 3D representation of the current city (2017), (d) 3D representation of the city for 2050.

REFERENCES

Biljecki, F., Stoter, J., Ledoux, H., Zlatanova, S. and Çöltekin, A. (2015). *Applications of 3D City Models: State of the Art Review*. ISPRS Int. J. Geo-Inf. 2015, 4, 2842-2889; doi:10.3390/ijgi4042842

Billen, R., Carre, C., Delfosse, V., Hervy, B., Laroche, F., Lefèvre, D., Servières, M. and Ruymbeke, M. (2012). *3D historical models: the case studies of Liege and Nantes*. http://hdl.handle.net/2268/126687

Billen, R., Cutting-Decelle, Af., Marina, O., Duarte de Almeida, J., Caglioni, M., Falquet, G., Leduc, T., Métral, C., Moreau, G., Perret, J., Rabino, G., García, R., Yatskiv, I., and Zlatanova, S., (2014). *3D City Models and urban information: Current issues and perspectives*. 10.1051/TU0801/201400001.

Billen, R., Zaki, C., Servières, M., Moreau, G. and Hallot, P. (2012). *Developing an ontology of space: Application to 3D city modeling*. 02007. 10.1051/3u3d/201202007.

Chaturvedi, K., Yao, Z., & Kolbe, T. H. (2019). *Integrated management and visualization of static and dynamic properties of semantic 3D city models*. International Archives of the Photogrammetry, Remote Sensing & Spatial Information Sciences.

Clarke K. C. (2008). *A Decade of Cellular Urban Modeling with SLEUTH: Unresolved Issues and Problems*. In Brail R.-K. (eds.), Planning Support Systems for Cities and Region, Lincoln Institute of Land Policy, Cambridge, MA, 47–60.

EL Meouche, R., Rezoug, M., Hijazi, I. and Maes, D. (2013). *Automatic Reconstruction of 3D Building Models from Terrestrial Laser Scanner Data*. ISPRS Annals of Photogrammetry, Remote Sensing and Spatial Information Sciences. II-4/W1. 7-12. 10.5194/isprsannals-II-4-W1-7-2013.

Eslahi, M., (2019). *Simulations de croissance urbaine pour représenter les impacts possibles des constructions et des contraintes environnementales sur l'étalement urbain (Urban growth simulations in order to represent the impacts of constructions and environmental constraints on urban sprawl - Constructibility and application to urban sprawl)*, PhD diss., University of Paris Est, 2019.

Eslahi, M., El Meouche, R., and Ruas, A. (2019). *Using building types and demographic data to improve our understanding and use of urban sprawl simulation*, Proc. Int. Cartogr. Assoc., 2, 28, https://doi.org/10.5194/ica-proc-2-28-2019, 2019.

Haala, N., Kada, M., (2010). *An update on automatic 3D building reconstruction*. ISPRS Journal of Photogrammetry and Remote Sensing. 65. 570-580. 10.1016/j.isprsjprs.2010.09.006.

Hervy, B., Billen, R., Laroche, F., Carre, C., Servières, M., Ruymbeke, M., Tourre, V., Delfosse, V. and Kerouanton, J. L. (2012). *A generalized approach for historical mock-up acquisition and data modelling: Towards historically enriched 3D city models*. 02009. 10.1051/3u3d/201202009.

Kapoor, M., Khreim, J.F., El Meouche, R., Bassit, D., Henry, A., Ghosh, S. (2010). *Comparison of techniques for the 3D modeling and thermal analysis*. x Congreso Internacional Expresión Gráfica aplicada a la Edificación Graphic Expression applied to Building International Conference, APEGA 2010

Kolbe, T.H. and Gröger, G. (2003). *Towards unified 3D city models*. In Proceedings of the ISPRS Commission IV Joint Workshop on Challenges in Geospatial Analysis, Integration and Visualization II, Stuttgart, Germany, 8–9 September 2003.

Ledoux, H. and Meijers, M. (2011). *Topologically consistent 3D city models obtained by extrusion*. Int. J. Geogr. Inf. Sci. 2011, 25, 557–574.

Pedrinis, Frédéric and Gesquière, Gilles. (2017). *Reconstructing 3D Building Models with the 2D Cadastre for Semantic Enhancement*. 10.1007/978-3-319-25691-7_7.

Pepe, M., Fregonese, L., & Crocetto, N. (2019). *Use of SfM-MVS approach to nadir and oblique images generated through aerial cameras to build 2.5D maps and 3D models in urban areas*, Geocarto International. 1-17, DOI: 10.1080/10106049.2019.1700558

Project Gigalopolis. (2018). *http://www.ncgia.ucsb.edu/*

Shiode, N. (2000). *3D urban models: Recent developments in the digital modelling of urban environments in three-dimensions*. GeoJournal. 52. 263-269. 10.1023/A: 1014276309416.

Tomljenovic, I., Höfle, B., Tiede, D. and Blaschke, T. (2015). *Building Extraction from Airborne Laser Scanning Data: An Analysis of the State of the Art*. Remote Sensing. 7. 3826-3862. 10.3390/rs70403826.

Zhu, Q., Hu, M., Zhang, Y. and Du, Z. (2009). *Research and practice in three-dimensional city modeling*. Geo-spatial Information Science. 12. 18-24. 10.1007/s11806-009-0195-z.